buildings

MDPI

Article

Study on Mechanical Properties and Safety of Ultra-Thin Reactive Powder Concrete Prefabricated Slabs Applied to I-Beam Joints of Bridges

Bin Liu [1], Xiang Liu [2], Buyu Jia [2,*], Quansheng Yan [2] and Zheng Yang [2]

[1] Poly Changda Engineering Co., Ltd., Guangzhou 510630, China; cdliubin@polycd.com
[2] School of Civil Engineering and Transportation, South China University of Technology, Guangzhou 510641, China; 202421008657@mail.scut.edu.cn (X.L.); cvqshyan@scut.edu.cn (Q.Y.); ctyz@scut.edu.cn (Z.Y.)
* Correspondence: ctjby@scut.edu.cn

Abstract: Conventional methods for constructing bridge I-beam joints face several challenges, including heavy precast slabs, complicated transportation and lifting procedures, strict accuracy requirements, lengthy construction timelines, and increased safety risks. The use of ultra-thin, high-performance reactive powder concrete (RPC) prefabricated slabs can effectively resolve these issues. However, research in this area is limited, leaving our understanding of the strength and feasibility of ultra-thin RPC slabs for I-beam joints incomplete. Therefore, this study conducts a thorough examination of the strength and safety aspects of these slabs to assess their practical suitability. First, 11 numerical models are generated to evaluate the bearing capacity of ultra-thin RPC slabs, determining key factors such as cracking load, ultimate load, and safety factor according to relevant codes and standards. This establishes a theoretical foundation for practical engineering applications. Next, several sets of ultra-thin RPC slabs that meet material performance criteria are prefabricated to study the mechanical properties under equivalent concentrated load. Finally, two types of in situ temporary construction loads are encountered in the safety calculations of the RPC slabs. This study aims to provide a robust theoretical framework and technical support for the application and advancement of ultra-thin RPC prefabricated slabs in bridge I-beam joints.

Keywords: bridge construction; I-beam joint; reactive powder concrete (RPC); ultra-thin RPC prefabricated slab; numerical analysis; experimental test

Citation: Liu, B.; Liu, X.; Jia, B.; Yan, Q.; Yang, Z. Study on Mechanical Properties and Safety of Ultra-Thin Reactive Powder Concrete Prefabricated Slabs Applied to I-Beam Joints of Bridges. *Buildings* **2024**, *14*, 3456. https://doi.org/10.3390/buildings14113456

Academic Editor: Fabrizio Gara

Received: 27 September 2024
Revised: 15 October 2024
Accepted: 22 October 2024
Published: 30 October 2024

1. Introduction

In bridge construction, joining I-beams is a critical phase. Traditionally, three primary methods are employed to manage I-beam joints [1,2]: reinforced concrete prefabricated slab pavement, a full support bottom formwork cast in place, and cast-in-place concrete using hanging molds. Reinforced concrete prefabricated slab pavement is widely used due to its advantages in factory-standardized production, easy quality control, fast on-site installation, and reduced construction time. However, this approach has drawbacks, including the heavy weight of prefabricated slabs, complex transportation and lifting, and the need for precise on-site accuracy for proper overlap.

Alternatively, using steel formwork allows for flexible, cast-in-place concrete wet joints. This method is adaptable for various complex bridge structures and ensures reliable joint quality. However, it requires significant manpower and materials, lengthens construction timelines, and imposes stricter construction conditions. The cast-in-place method involves several steps, including lifting rectangular bottom molds, binding steel, placing concrete, and removing formwork. This method tends to be complicated, incurs high personnel and machinery costs, and carries increased safety risks.

To overcome the limitations of traditional methods, innovative materials such as reactive powder concrete (RPC), ultra-high-performance concrete (UHPC), and Fiber-Reinforced Polymers (FRPs) have been introduced in bridge joint construction. These materials offer impressive durability, lightweight properties, and high tensile strength, which enhance construction efficiency, cost-effectiveness, and the overall lifespan of joints. However, when considering temporary construction loads (like worker and light machinery weights) and economic feasibility, the use of high-strength but expensive materials like UHPC and FRPs becomes less practical. In contrast, RPC prefabricated slabs serve as a competitive alternative. RPC is a novel high-performance concrete that optimizes particle composition [3–8], incorporates active powders, and is reinforced with steel fibers, significantly improving both compressive and tensile strengths [9,10]. Its application as I-beam joint slabs effectively reduces dead weight [11,12], minimizes dimensions while maintaining strength, lowers costs, and promotes eco-friendly construction [13,14]. Furthermore, RPC's dense microstructure provides excellent impermeability and corrosion resistance, highlighting its potential in bridge engineering.

Current research on RPC in bridge construction mainly focuses on structural reinforcement and deck paving, showing its ability to enhance flexural and shear capacities, thus extending the service life of bridges [15–18]. RPC has gained attention for reinforcing existing bridges; strategically incorporating RPC layers can revitalize the structural integrity and performance of older bridges, boosting their load-bearing capacity and mitigating stress exceedances [19]. In bridge deck applications, RPC demonstrates exceptional crack resistance and durability, effectively addressing deck cracking issues [20]. However, studies on RPC prefabricated slabs in beam-to-beam joints are limited, primarily focusing on durability [21,22].

At present, there is a lack of research on the mechanical properties of RPC prefabricated slabs, especially ultra-thin varieties, in beam joint applications. To validate the practical effectiveness of these RPC slabs in real-world projects, this study integrates numerical simulations, theoretical analyses, and component loading experiments tailored to engineering scenarios [23]. We investigate the mechanical characteristics of ultra-thin RPC prefabricated slabs, considering variations in size, strength, and material composition. These findings will strengthen the technical basis for adopting ultra-thin RPC prefabricated slabs in I-beam joint applications, advancing bridge engineering practice.

2. Project Overview

The primary superstructure of the eastern outer ring highway bridge in the city consists of 18,703 pieces of pretensioned I-beams, with spans ranging from 20 to 40 m. The standard specifications for these I-beams include a belly width of 20 cm, a flange thickness of 14 cm, a top width of 2.05 m, and a bottom width of 1 m. A representative cross-section of the 35 m span is shown in Figure 1.

Each span contains seven beam seams, with seam widths varying from 140 mm to 1100 mm, and a standard seam width of 550 mm. An innovative aspect of this design is the use of ultra-thin RPC prefabricated slabs, which replace the conventional reinforced concrete prefabricated slab design. For brevity, the term "RPC slab" will refer to these ultra-thin RPC slabs.

The RPC slabs have fixed dimensions of 1000 mm in length and 20 mm in thickness (as depicted in Figure 2). Given the varying beam joint widths, which range from 140 mm to 1100 mm, the widths of the RPC slabs also vary, spanning from 240 mm to 1200 mm. Notably, the most common slab widths are 650 mm, 900 mm, and 1200 mm, which account for a significant portion of the total.

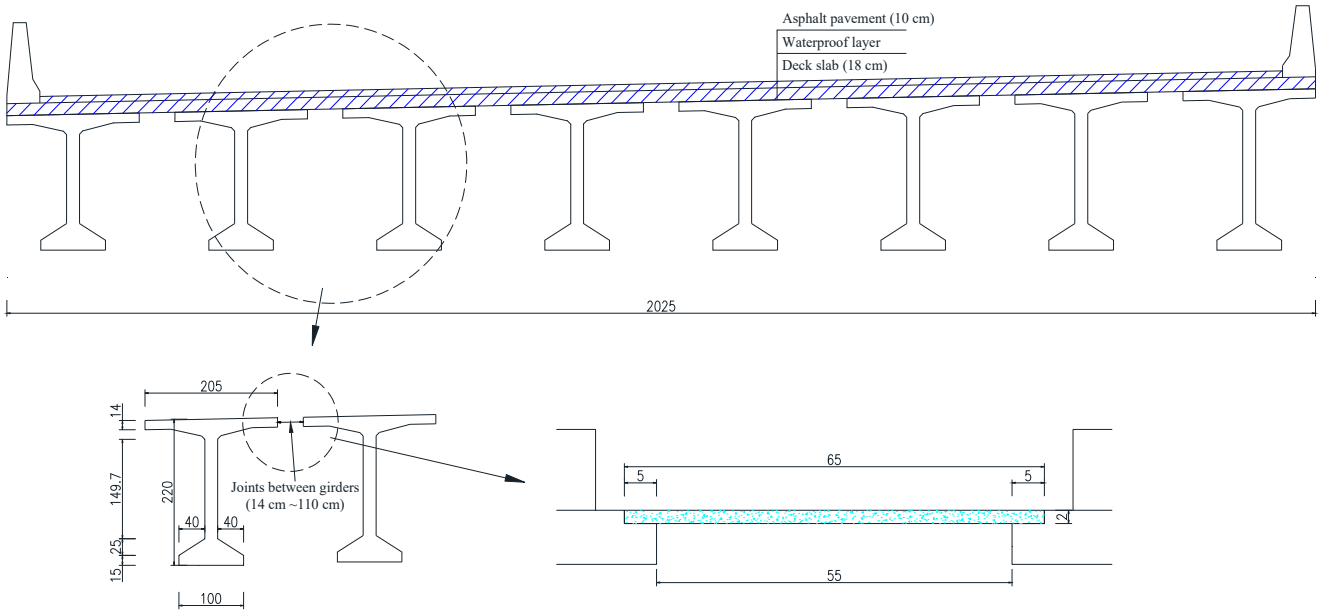

Figure 1. Schematic diagram of joint of I-beam (unit: cm).

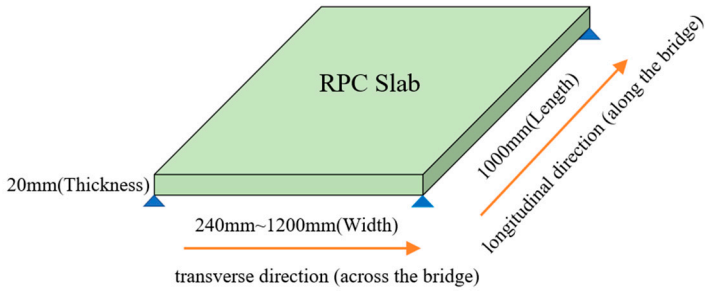

Figure 2. Typical shape form of the RPC slab unit.

3. Bearing Capacity Beads on a Numerical Analysis of RPC Slab Unit

3.1. Numerical Simulation

Finite element analysis was performed using Abaqus/Explicit 2020, a leading software for large-scale computational simulations in engineering. This analysis included several stages: creating geometric components, specifying material properties, assembling the specimens, outlining the analysis steps, establishing contact interactions, applying loads, generating the mesh, and conducting post-processing. The plastic damage model (CDP) in ABAQUS was used to simulate the behavior of reactive powder concrete (RPC), accounting for both compressive and tensile properties, as shown in Figure 3.

The numerical simulations focused on three widths of RPC slabs (beam gap spans), 650 mm, 900 mm, and 1200 mm, with fixed values for length and thickness at 1000 mm and 20 mm, respectively. Four compressive strengths were considered for the RPC slabs, 100 MPa, 120 MPa, 140 MPa, and 160 MPa, with corresponding tensile strengths of 5.5 MPa, 6.7 MPa, 7.9 MPa, and 9.0 MPa. These strengths will be denoted as C100, C120, C140, and C160.

An eight-node linear reduced integration element (C3D8R) was employed for the simulation of the RPC slabs. After comparing mesh sizes of 5 mm, 7 mm, 8 mm, 9 mm, and 10 mm, a mesh size of 7 mm was selected to balance computational efficiency and accuracy. The RPC slabs were simply supported at both ends, with left boundary conditions of (UY = 0, UZ = 0) and right boundary conditions of (UY = 0). Node constraints were applied to all nodes on the support lines. The numerical models for the 650 mm, 900 mm,

and 1200 mm slab widths are illustrated in Figure 4. The loading mode considered is both concentrated and uniform loading.

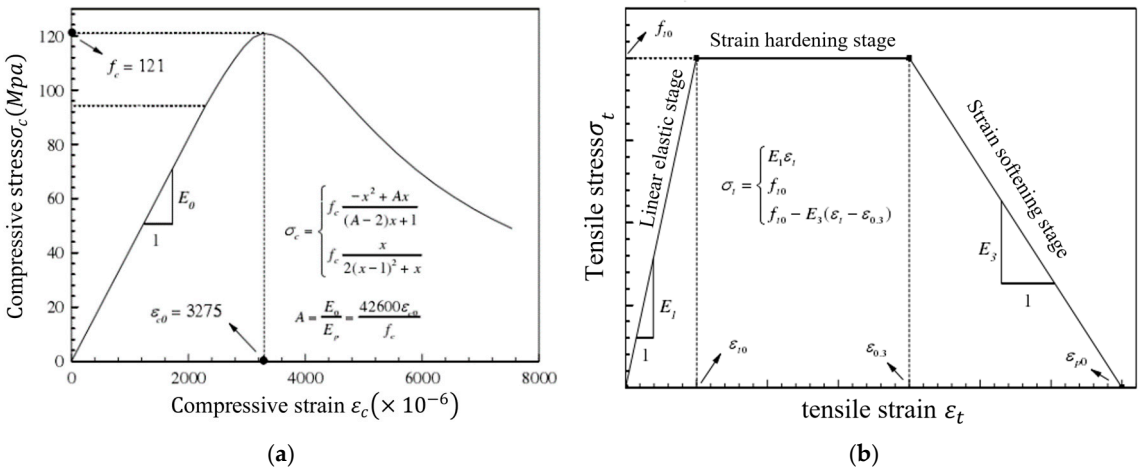

Figure 3. Constitutive relation of RPC: (**a**) Compression constitutive; (**b**) tension constitutive.

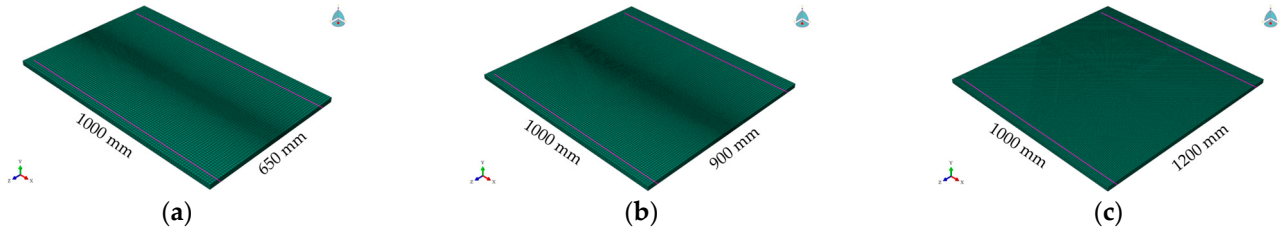

Figure 4. Numerical model: (**a**) Slab width 650 mm; (**b**) slab width 900 mm; (**c**) slab width 1200 mm.

3.2. Numerical Simulation Analysis of the Load-Bearing Capacity of RPC Slabs

The steel fiber in the RPC material was set at 2%, with a length-to-diameter ratio = 13 mm to 2 mm. The analysis focused on three main slab widths, 650 mm, 900 mm, and 1200 mm, with RPC strength grades of C100, C120, and C140. Additionally, the strength class C160 was calculated and analyzed for the 900 mm and 1200 mm wide slabs. The ultimate load simulation results under various conditions are presented in Figures 5 and 6. For instance, W650-C100-CL (or DL) indicates a slab width of 650 mm, a strength level of C100, and a concentrated load (or uniform load).

The results indicate that the ultimate load of the RPC slab increases with higher strength grades. However, as the slab width increases, the ultimate load rapidly decreases. Therefore, when using wider RPC slabs, it is crucial to consider employing RPC with a higher strength grade. This analysis provides insights into the ultimate bearing capacity, but practical applications also require the consideration of normal load capacity and cracking load estimates.

This study aims to estimate the cracking load using the element stress damage factor, DAMAGET, in ABAQUS, which represents the tensile damage index of concrete. When DAMAGET exceeds 0, the concrete is considered to have cracked. Figure 7 illustrates the failure progression of the RPC slab. During the initial loading phase, the concrete at the bottom of the slab remains in the linear elastic stage, exhibiting minimal tensile strain and no damage, resulting in a DAMAGET index of 0. As the load increases, the concrete transitions into the strain-hardening phase, where tensile strain rises rapidly and damage begins, evident in the decline in the elastic modulus and an increase in the DAMAGET index.

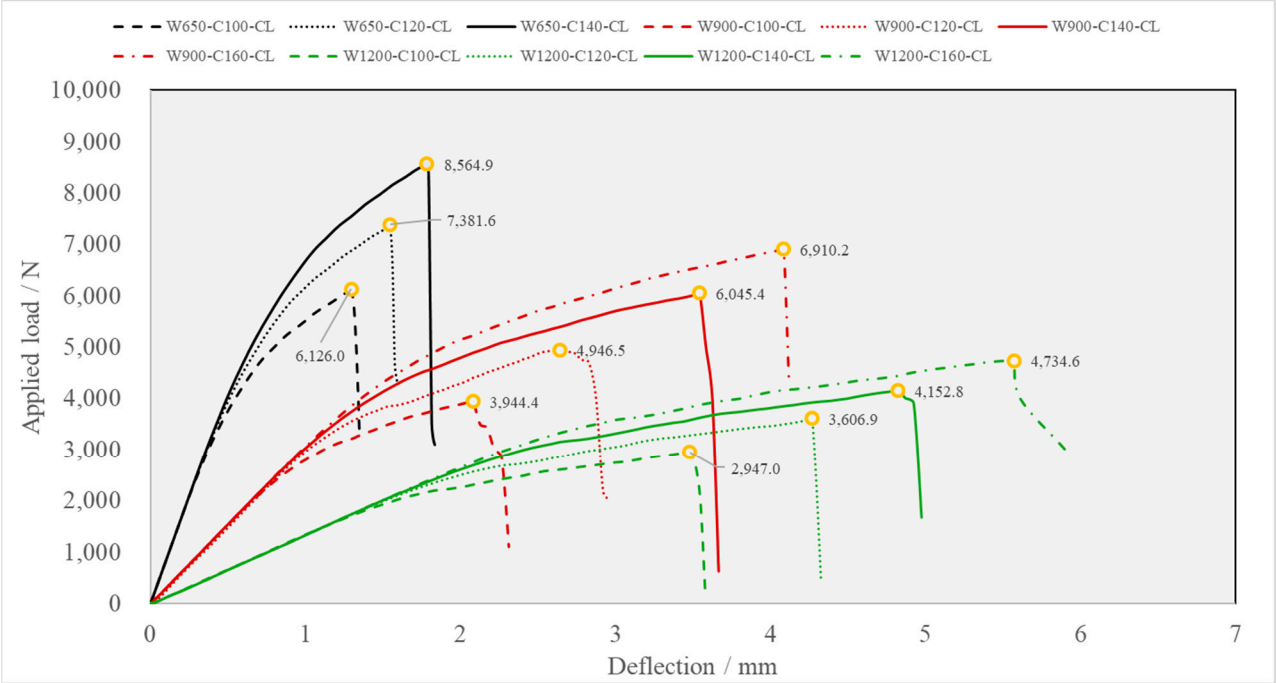

Figure 5. $F-\Delta$ curve under concentrated load.

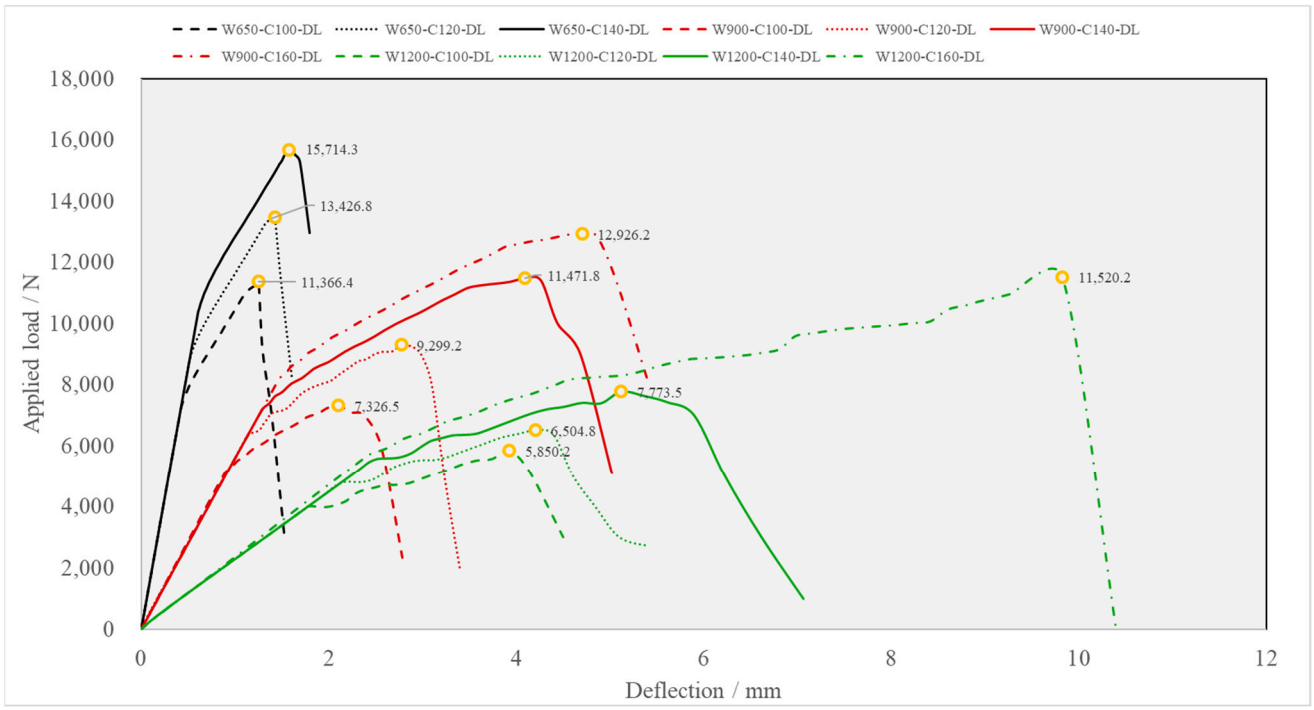

Figure 6. $F-\Delta$ curve under uniformly distributed load.

As loading continues, the damaged area at the bottom of the slab expands quickly, intensifying damage in the mid-span region. Consequently, the DAMAGET index increases, ultimately reaching the maximum damage threshold of 0.9065, as set by the finite element model (indicated by the red zone in the damage contour plot). At this point, the bearing capacity of the concrete slab peaks, signifying failure.

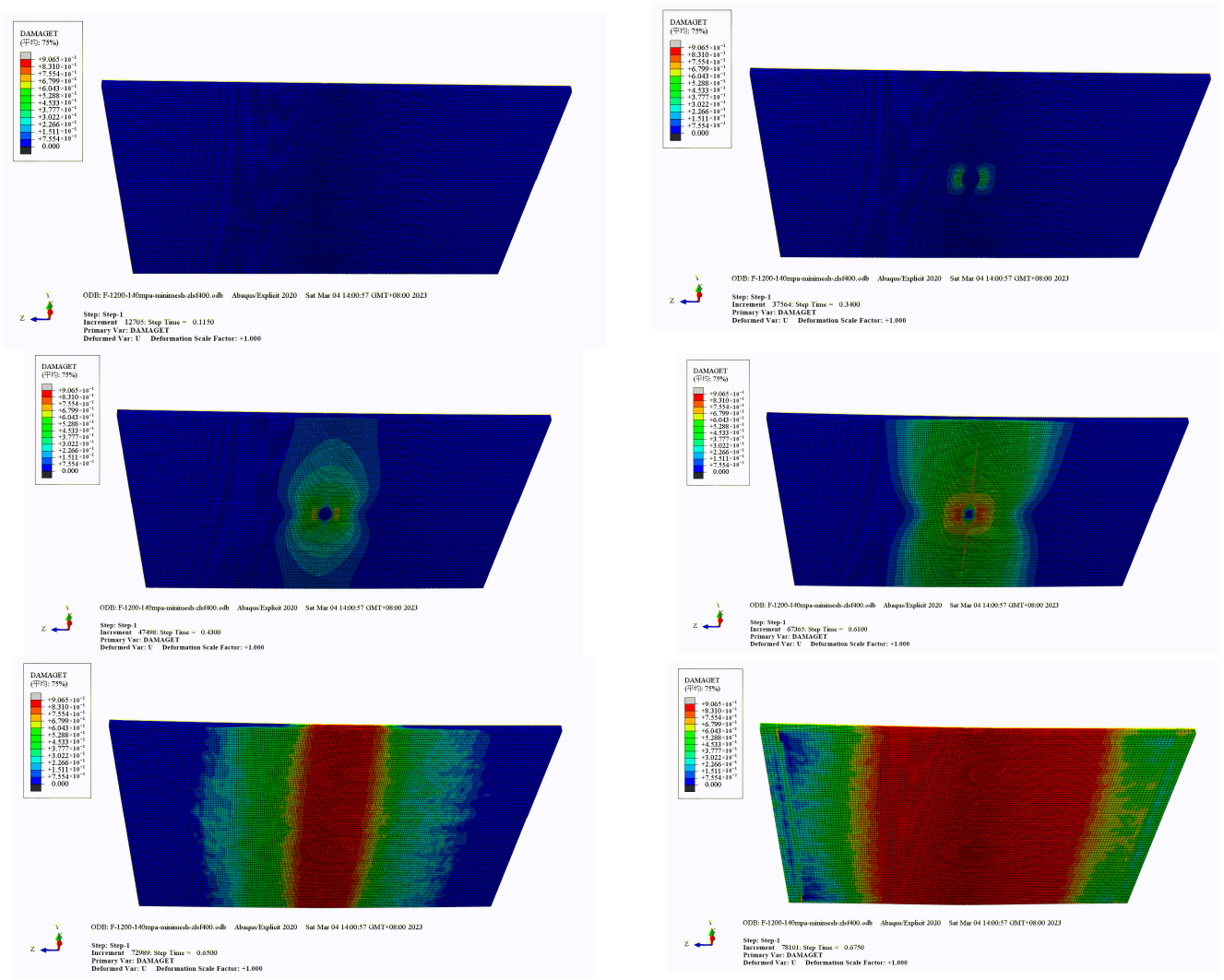

Figure 7. Numerical failure process of RPC slab.

3.3. Safety Analysis of RPC Slabs

Table 1 summarizes the cracking loads and ultimate loads of RPC slabs with varying dimensions (specifically, slab widths) and strengths. Currently, there are no established specifications outlining the performance criteria for I-beam joint RPC slabs. Therefore, this study references the specifications in "Railway Cable Trough Cover Slab and Sidewalk Slab—Part 1: Reactive Powder Concrete Type" for safety assessment and calculations. The load-bearing capacity of RPC slabs must meet the requirements to withstand a concentrated load of 1.5 kN and a uniform load of 5 kN/m².

To quantify the safety margin of RPC slabs, a dimensionless surplus coefficient is introduced, calculated as the ratio of the cracking or ultimate load to the stipulated standard load. Specifically, the coefficients are defined as follows:

(1) Residual coefficient for concentrated force cracking I_c and excess coefficient of ultimate load I_u:

$$I_c = \frac{CF_{crack}}{1.5}, \quad I_u = \frac{CF_{cu}}{5} \tag{1}$$

(2) Uniform bursting surplus coefficient P_c and excess coefficient of ultimate load P_u:

$$P_c = \frac{DF_{crack}}{1.5}, \quad P_u = \frac{DF_{cu}}{5} \tag{2}$$

Here, CF_{crack} and CF_{cu} represent the cracking load and ultimate load of an RPC slab under concentrated force, respectively, while DF_{crack} and DF_{cu} represent the corresponding values under uniform force. The cracking and limit margin coefficients of the RPC slab are shown in Table 1 and Figure 8.

Table 1. The load-bearing performance of RPC slabs.

Width of Slab/mm	RPC Intensity	Concentrated Force Action				Uniform Force Action			
		Cracking Load/kN	Ultimate Load/kN	Cracking Surplus Coefficient	Limiting Margin Coefficient	Cracking Load/kN	Ultimate Load (kN/m^2)	Cracking Surplus Coefficient	Limiting Margin Coefficient
650	C100	1.91	6.13	1.28	4.08	13.25	20.67	2.65	4.13
650	C120	2.30	7.38	1.54	4.92	16.12	24.48	3.22	4.90
650	C140	2.73	8.56	1.82	5.71	19.11	28.57	3.82	5.71
900	C100	1.43	3.94	0.96	2.63	4.99	9.16	1.00	1.83
900	C120	1.70	4.95	1.13	3.30	7.70	11.62	1.54	2.32
900	C140	2.12	6.05	1.41	4.04	8.88	14.34	1.78	2.87
900	C160	2.51	6.91	1.67	4.61	10.01	16.16	2.00	3.23
1200	C100	1.06	2.95	0.70	1.96	3.15	5.32	0.63	1.06
1200	C120	1.23	3.61	0.82	2.4	3.29	5.91	0.66	1.18
1200	C140	1.47	4.15	0.98	2.77	4.49	7.07	0.90	1.41
1200	C160	1.72	5.19	1.14	3.46	5.06	10.47	1.01	2.09

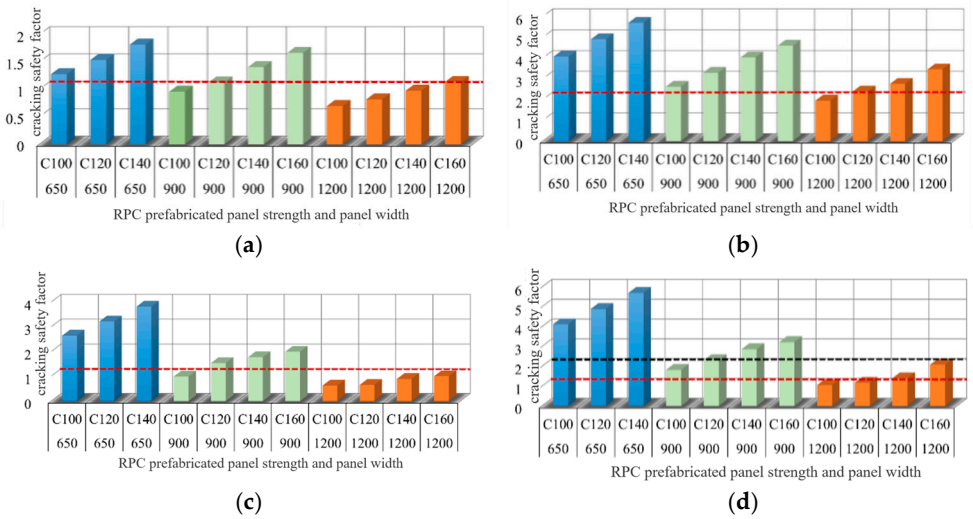

Figure 8. Cracking and ultimate margin coefficients of RPC slabs: (**a**) Cracking surplus coefficient under concentrated force; (**b**) limiting coefficient of excess under concentrated force; (**c**) the cracking surplus coefficient under uniform distribution force; (**d**) the limiting surplus coefficient under uniform distribution force.

To ensure that RPC slabs provide adequate safety margins in practical applications, it is crucial that they meet not only the prescribed ultimate load capacity requirements but also the criteria for normal service loads. To achieve this, specific safety standards can be established as follows:

$$min(I_c, P_c) \geq 1, \quad min(I_u, P_u) \geq 2 \tag{3}$$

This means that the cracking surplus coefficient (for both concentrated and uniform loads) should be no less than 1, and the limiting surplus coefficient (for both types of loads) should be no less than 2.

From Table 1 and Figure 8, we can conclude the following:

(1) For both concentrated and uniform loads, the minimum strength grade C100 corresponds to a cracking surplus coefficient greater than 1, and the ultimate load coefficient is close to 4. Thus, when the slab width is 650 mm, the C100 strength grade RPC slab meets the specified safety standards.
(2) When the slab width is 900 mm, the C100 strength grade no longer meets the requirements; the strength grade of at least C120 is needed.
(3) For a slab width of 1200 mm, a minimum strength grade of C160 is required.

These results should not be seen as definitive criteria for engineering selections, as project managers may prefer higher safety benchmarks. For instance, RPC slabs with widths of 650 mm or 900 mm might consider using the C140 strength grade.

3.4. Experimental Test

To validate the mechanical properties of RPC slabs, a comprehensive series of loading experiments was systematically conducted on specimens subjected to various operational conditions. The mix proportions for these specimens are detailed in Table 2. All specimens were uniformly blended with 13 mm short straight fibers, which made up 2% of the total mixture.

Table 2. Material mix ratio of test specimens.

Volume/W	Strength Class	Cement PII/kg	Silica Fume /kg	Mineral Powder (95 Rank)/kg	Fly ash Class I /kg	Machine-Made Sand/kg	Water/kg	Admixture/kg	Water kg/W	Water-Reducing Agent kg/W
1000	C140	720	206	93	90	1000	183	25.507	0.183	0.026
1000	C160	720	220	80	60	1030	178	27	0.178	0.027

Initially, multiple groups of material strength experiments were performed (see Figure 9) to establish the strength indexes of the specimens: compressive strength, tensile strength, and flexural strength. Following thorough experimental analysis and material refinement, the differences between the experimentally determined and designed values for strength grades C100, C120, C140, and C160 were carefully controlled, maintaining a deviation threshold of no more than 2%.

(**a**) (**b**) (**c**)

Figure 9. Strength tests: (**a**) Compression test; (**b**) tensile test; (**c**) bending test.

For the loading apparatus, a concentrated approach utilizing single-point loading methodology was employed. As illustrated in Figure 10a,b, the device incorporated a reversed loading configuration, with the bottom of the RPC slab facing upwards. This orientation allowed for the direct observation of surface cracking under strain. A loading slab, measuring 60 mm × 60 mm × 20 mm, was placed between the jack and the prefabricated slab.

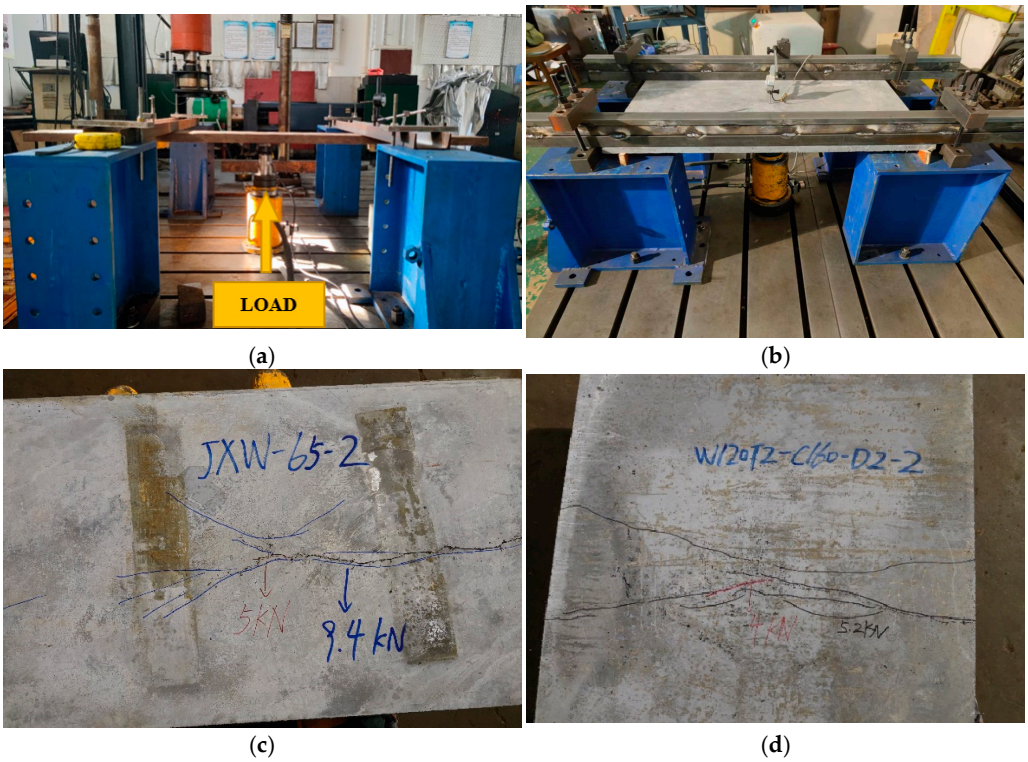

Figure 10. Loading test and test specimens: (**a**) Concentrated loading diagram; (**b**) RPC slab test site; (**c**) 650 mm slab width + C140 RPC slab; (**d**) 1200 mm slab width + C160 RPC slab.

Due to spatial constraints, experimental data from the 650 mm and 1200 mm RPC slabs were selected for analysis. For clarity, the specimen numbering method is as follows: Wn indicates a slab width of n, Cn indicates a strength grade of n, and [n] represents the NTH sample. For example, W65-C140-[1] denotes the first RPC slab with a width of 650 mm and a material strength class of C140. Figure 10c,d show the two types of RPC slab specimens: 650 mm with C140 and 1200 mm with C160.

Table 3 presents the experimental results regarding the concentrated loading performance of RPC slabs with varying widths (650 mm + C140 strength grade and 1200 mm + C160 strength grade). Analysis of Table 3 indicates that for the 650 mm wide slabs with a C140 strength grade, the cracking load exceeded 1.5 kN across all specimens, with a minimum ultimate load of 7.8 kN. In contrast, when the slab width increased to 1200 mm and the strength grade rose to C160, all specimens demonstrated cracking loads greater than 1.5 kN, although the minimum ultimate load decreased to 5.1 kN. These experimental findings confirm the robustness of the mechanical properties of RPC slabs.

Table 3. Results of concentrated loading tests for RPC prefabricated slabs.

Test Piece	Cracking Load /kN	Ultimate Load /kN	Ductility Coefficient	Mean Cracking Load/kN	Mean Limit Load/kN
W650-C140-[1]	5.0	9.6	1.92		
W650-C140-[2]	4.1	8.7	2.12		
W650-C140-[3]	4.6	8.9	1.93	4.38	8.76
W650-C140-[4]	4.2	7.8	1.86		
W650-C140-[5]	4.0	8.8	2.20		
W1200-C160-[1]	4.0	5.2	1.30		
W1200-C160-[2]	3.5	5.1	1.46		
W1200-C160-[3]	3.0	4.8	1.60	3.52	5.22
W1200-C160-[4]	3.9	5.8	1.49		
W1200-C160-[5]	3.2	5.2	1.63		

A comparison of the experimental results with those from numerical simulations (as shown in Table 3) reveals that the experimental cracking loads exceeded the numerical simulation results, while the ultimate load ratios were closer to the simulation values.

4. Safety Check of Temporary Construction Loads

The analysis presented above primarily addresses specification requirements and does not encompass all safety considerations necessary for actual projects. In the context of the background project, it is essential to conduct safety checks for the temporary construction loads that exist on-site. This involves focusing on the following two specific load conditions for safety calculations:

(1) Temporary Load Condition 1—Worker Standing on RPC Slabs: During the installation of the prefabricated slab between the I-beams, safety checks should account for the weight of three workers standing in the middle of the slab.
(2) Temporary Load Condition 2—Pavement Layer Construction: While constructing the pavement layer, safety checks must consider the combined weight of construction workers and the pavement layer load acting on the precast RPC slab.

4.1. Safety Check of Temporary Loads from Workers Standing on RPC Slabs

Considering the simultaneous loading of three workers, each weighing 75 kg, the load was applied at mid-span under the most unfavorable conditions. The combined load of the three workers was equivalent to that on a 500 mm × 500 mm slab. The analysis focused on three types of RPC slabs, W650-C140, W900-C160, and W1200-C160, with a standard thickness of 20 mm. The results of the safety check are shown in Table 4. As indicated, the RPC slabs in all three categories will not crack when three workers stand on them.

Table 4. Safety results of workers standing temporary load.

RPC Slab Type	Slab Thickness/mm	DAMAGET Index	Maximum Principal Tensile Stress of RPC Slab/MPa	Cracking or Not	Whether the Limit Load Is Reached
W650-C140	20	<0	2.29	No	No
W900-C160	20	<0	3.98	No	No
W1200-C160	20	<0	5.89	No	No

4.2. Safety Check of Temporary Load of Pavement Layer Construction

During the construction of a pavement layer, a reinforcing mesh is placed atop the prefabricated RPC slabs, with construction workers standing on this mesh while pouring concrete. The weight of the workers can be considered as a uniform surface load. According to the standard crowd load values specified in Table 4.3.1 of the "General Code for Engineering Structures—GB 55001-2021" [24], the working load of the construction workers during concrete pouring is equivalent to a uniformly distributed load of 3 kN/m². The combined weight of the pavement layer and the RPC slab results in a uniformly distributed load of 5 kN/m².

Five types of RPC slabs were selected for this analysis: W650-C140, W900-C160, W1000-C160, W1100-C160, and W1200-C160. The thicknesses of these slabs were varied, considering standard thicknesses of 20 mm, 25 mm, and 30 mm. The calculation results are presented in Table 5. From the data, it is evident that neither W650-C140 nor W900-C160 exhibited cracking at a thickness of 20 mm. However, W1000-C160 experienced cracking at 20 mm thickness but remained intact when it was increased to 25 mm. Similarly, W1100-C160 cracked at 20 mm thickness but was unaffected at 25 mm. For W1200-C160, cracking occurred even at 25 mm thickness, but increasing the thickness to 30 mm prevented further cracking.

Table 5. Safety results of temporary load during pavement construction.

RPC Slab Type	Slab Thickness/mm	DAMAGET Index	Maximum Principal Tensile Stress of RPC Slab /MPa	Cracking or Not	Whether the Ultimate Bearing Capacity Is Reached
W650-C140	20	<0	4.42	No	No
W900-C160	20	<0	8.60	No	No
W1000-C160	20	<0	9.97	Yes	No
W1000-C160	25	<0	7.58	No	No
W1100-C160	20	>0	9.99	Yes	No
W1100-C160	25	<0	9.40	No	No
W1200-C160	20	>0	11.26	Yes	No
W1200-C160	25	>0	9.96	Yes	No
W1200-C160	30	<0	7.56	No	No

5. Discussion

By setting reasonable material characteristic parameters in the ABAQUS numerical model, the numerical results of this paper agree well with the experimental results of the RPC slabs. This shows that it is feasible for the ABAQUS model to be used in the design phase of engineering projects. Firstly, a small number of material experiments were set to verify the accuracy of ABAQUS models, and then, the calculation of different design loads was carried out to optimize the design parameters such as the width and thickness of RPC slabs.

Based on the actual project, numerical theoretical research and component loading experimental analyses were carried out systematically to study the mechanical properties of ultra-thin RPC prefabricated panels with different sizes, strengths, and materials. The results can provide solid technical support for the application of ultra-thin RPC prefabricated slabs in the joints between I-beams of bridges.

The limitations of this study lie in the following two aspects: firstly, design and analysis based on the elastic state of the RPC slabs. If the performance of the slabs in the plastic working state is further excavated, the cost savings of this material are expected to be further exploited. Secondly, in the numerical simulation analysis, the boundary condition is ideally set as the simply supported mode. Although the numerical analysis results are in good agreement with the experimental results, there is still room for further detailed research.

6. Conclusions

The application of ultra-thin RPC prefabricated slabs to I-beam bridge joints effectively addresses the shortcomings of current technical solutions. To clarify the mechanical properties and engineering feasibility of these slabs, this research has focused on understanding their performance and safety through numerical simulations and experimental tests. The key findings with practical engineering value are summarized as follows:

(1) The numerical analysis of load-bearing capacity has determined the cracking and ultimate loads for ultra-thin RPC prefabricated slabs of different widths and strength grades. The results indicate that for a slab width of 650 mm, an RPC slab with a C100 strength grade meets the specified safety standards. When the slab width increases to 900 mm, a minimum strength grade of C120 is required. For a width of 1200 mm, a minimum strength grade of C160 is necessary.

(2) The experimental test results indicate that the RPC (reactive powder concrete) slabs produced with the proposed mix proportions demonstrate excellent mechanical properties. Notably, the experimental outcomes exceed those of the numerical simulations, showing significantly higher cracking loads and closely comparable ultimate loads.

(3) To ensure adequate safety margins for RPC (reactive powder concrete) slabs during construction, two primary types of temporary loads were considered: worker standing

loads and loads from temporary pavement layer construction. The findings indicate that the W650-C140, W900-C160, and W1200-C160 RPC slabs can support the weight of three workers without cracking. For the temporary loads associated with pavement layer construction, the W650-C140 and W900-C160 slabs with a thickness of 20 mm remain uncracked. However, the W1000-C160 and W1100-C160 slabs require an increase in thickness to 25 mm to prevent cracking, while the W1200-C160 slab necessitates a thickness enhancement to 30 mm.

Despite the advancements made in this study, several limitations remain that warrant further research. Firstly, this study only investigates the effect of 13 mm short straight fibers at a dosage of 2%, without exploring other dosages or fiber types (such as long fibers, end-hooked fibers, and glass fibers) that could optimize the mechanical properties of RPC slabs. Secondly, the focus has been solely on the safety evaluation of temporary construction loads, neglecting the impact of operational loads during the service life (e.g., potential shock effects from vehicular loads) and the long-term durability of RPC slabs. These issues highlight the need for more in-depth investigations to address these gaps and enhance the understanding and application of RPC slabs in civil engineering.

Author Contributions: Conceptualization, B.L. and X.L.; methodology, B.L.; software, Z.Y.; validation, B.J. and X.L.; formal analysis, Z.Y.; investigation, Q.Y.; resources, B.L.; data curation, B.J.; writing—original draft preparation, X.L.; writing—review and editing, Q.Y.; visualization, Z.Y.; supervision, Q.Y.; project administration, B.J.; funding acquisition, Z.Y. All authors have read and agreed to the published version of the manuscript.

Funding: This work was supported by the Natural Science Foundation of Guangdong Province, 550, China (Nos. 2022A1515011703 and 2022A1515011023).

Data Availability Statement: The original contributions presented in the study are included in the article, further inquiries can be directed to the corresponding author.

Conflicts of Interest: Author Bin Liu was employed by the company Poly Changda Engineering Co., Ltd. The remaining authors declare that the research was conducted in the absence of any commercial or financial relationships that could be construed as a potential conflict of interest.

References

1. Li, S. The comparison of construction methods of bridge deck system wet joints. *Shanxi Archit.* **2012**, *38*, 183–184+215. [CrossRef]
2. Song, X. Study on construction technology of bridge deck system and ancillary facilities. *Traffic World* **2021**, *30*, 32–33. [CrossRef]
3. Wu, Y.; He, Y. Experimental research on proportion of reactive powder concrete. *China J. Highw. Transp.* **2003**, *4*, 45–50. [CrossRef]
4. Liu, M.; Dai, W.; Zhong, C.; Yang, X. Study on mechanical properties and microstructure of manufactured sand reactive powder concrete with different curing methods. *Mater. Lett.* **2023**, *335*, 133818. [CrossRef]
5. Yan, Z.; An, M.; Zhong, T.; Ziruo, Y. Optimization Design Study of Railway Reactive Powder Concrete Bridge. *China Railw. Sci.* **2009**, *30*, 38–42. [CrossRef]
6. Shao, X.; Pan, R.; Zhan, H.; Fan, W.; Yang, Z.; Lei, W. Experimental verification of the feasibility of a novel prestressed reactive powder concrete box-girder bridge structure. *J. Bridge Eng.* **2017**, *22*, 04017015. [CrossRef]
7. Luo, H.; Ji, W.; Yan, Z.; Li, W. Research on Influence of Loading Methods on Compressive Behavior of Reactive Powder Concrete Filled Steel Tube Stub Columns under Axial Loads. *J. China Railw. Soc.* **2014**, *36*, 105–110.
8. Venkatesan, B.; Kannan, V.; Sophia, M. Utilization of granite powder and glass powder in reactive powder concrete: Assessment of strength and long-term durability properties. *Can. J. Civ. Eng.* **2022**, *49*, 885–898. [CrossRef]
9. Wang, Z.; Chen, S.; Jie, Y. Advance of research and application on reactive powder concrete. *Concrete* **2003**, *11*, 39–41+44.
10. Fang, Z.; Yang, J. Study and application of FRP and RPC in civil engineering. *J. Railw. Sci. Eng.* **2005**, *4*, 54–61. [CrossRef]
11. Dinler, E.; İpek, M. Impact Resistance of Sustainable Reactive Powder Concrete and Reinforced Concrete Slabs. *Cem. Wapno Beton* **2024**, *28*, 238–254. [CrossRef]
12. Mohammed, M.K.A. Performance of Reactive Powder Concrete slabs with different curing conditions. *J. Eng. Technol. Res.* **2014**, *6*, 81–93. [CrossRef]
13. Ju, Y.; Zhang, H.; Wang, D.; Kong, X.; Ma, Y.; Zhang, X.; Bai, J. Effect of mineral admixtures on the resistance to sulfate attack of reactive powder concrete. *J. Clean. Prod.* **2024**, *440*, 140769. [CrossRef]
14. Zhou, Y.; Luo, H.; Anand, K.; Singh, A.; Xie, Y.M. Sustainable use of ultrafine recycled glass in additive manufactured (3D printed) reactive powder concrete. *Constr. Build. Mater.* **2024**, *419*, 135556. [CrossRef]
15. Sajid, H.U.; Kiran, R. Effect of fiber reinforcement, mineral admixtures, and air entrainment on the fire performance of concrete in bridges: A review. *Constr. Build. Mater.* **2024**, *430*, 136420. [CrossRef]

16. Shah, H.A.; Yuan, Q.; Photwichai, N. Use of materials to lower the cost of ultra-high-performance concrete—A review. *Constr. Build. Mater.* **2022**, *327*, 127045. [CrossRef]
17. Marzoq, Z.H.; Borhan, T.M. Modelling hybrid reactive powder concrete T-beams. *J. Phys. Conf. Ser.* **2021**, *1895*, 012054. [CrossRef]
18. Nafees, A.; Javed, M.F.; Musarat, M.A.; Ali, M.; Aslam, F.; Vatin, N.I. FE Modelling and Analysis of Beam Column Joint Using Reactive Powder Concrete. *Crystals* **2021**, *11*, 1372. [CrossRef]
19. Fang, Z.; Chen, Z.; Chen, X.; Xiong, X. Comprehensive Treatment on Overstressed Compressive stress in Prestressed Concrete Continuous Box Girder Bridge. *Bridge Constr.* **2019**, *49*, 74–79.
20. Shao, X.; Chen, B.; Zhou, X. Experiment on Bending Behavior of Wet Joints in Light-weighed Composite Deck System Composed of Steel and RPC Layer. *China J. Highw. Transp.* **2017**, *30*, 210–217. [CrossRef]
21. Zhao, C.; Wang, K.; Zhou, Q.; Deng, K.; Cui, B. Full-scale test and simulation on flexural behavior of dovetail-shaped reactive powder–concrete wet joint in a composite deck system. *J. Bridge Eng.* **2018**, *23*, 04018051. [CrossRef]
22. Nassiraei, H. Probabilistic Analysis of Strength in Retrofitted X-Joints under Tensile Loading and Fire Conditions. *Buildings* **2024**, *14*, 2105. [CrossRef]
23. Yang, K.-J.; Xie, Z.-L.; Li, W. Application of RPC Constitutive Model in FEA. *Appl. Mech. Mater.* **2014**, *578–579*, 25–30. [CrossRef]
24. *GB 55001-2021*; General Code for Engineering Structures. Ministry of Housing and Urban-Rural Development: Beijing, China, 2021.